INSTITUTE OF PHYSICS PUBLISHING JOURNAL OF PHYSICS B: ATOMIC, MOLECULAR AND OPTICAL PHYSICS

J. Phys. B: At. Mol. Opt. Phys. **35** (2002) 2961–2974 PII: S0953-4075(02)31159-3

# A framework for understanding molecular ionization in strong laser fields

**Saipriya V Menon**[1], **John P Nibarger**[1,2] **and George N Gibson**[1]

[1] Department of Physics, University of Connecticut, Storrs, CT 06269, USA
[2] National Institute of Standards and Technology, Boulder, CO 80305, USA

E-mail: gibson@phys.uconn.edu

Received 23 November 2001, in final form 8 March 2002
Published 25 June 2002
Online at stacks.iop.org/JPhysB/35/2961

**Abstract**

The aim of this paper is to examine the role of excited states and multi-electron interactions in molecular ionization by strong laser fields. We present new data on the ionization and dissociation of iodine molecules that reveal important aspects of the strong field–molecule interaction in the short pulse regime. Our data, along with previous studies, is inconsistent with the simplest and commonly accepted model of molecular ionization in a strong laser field and this has led us to examine closely the individual ionization steps. We have found that a molecule can ionize into several distinct configurations predominantly through multi-electron interactions and the abundance of such configurations is dependent on internuclear separation. The ionization appears to be dominated by pairs of states with gerade and ungerade symmetry, as they have a large dipole coupling and the transition is near resonant with the strong laser field. In a one-electron molecule, this pair consists of the ground and first excited state whereas in a two-electron molecule this corresponds to the lowest lying pair of ionic states. In this paper, we propose a framework for organizing the numerous ionization pathways based on the electronic configuration of the initial charge state.

## 1. Introduction

One important goal of strong field physics is to better understand how electronic structure influences the matter–strong field interaction. These interactions are intricate and can involve multi-electron effects. To this end, atomic ionization has been studied [1] and electrons tunnelling out of the total field (Coulomb potential plus the laser electric field) to the continuum dominate the interaction. The ionization rates in atoms are typically described using the Ammosov–Delone–Krainov (ADK) tunnelling model [2]. This relatively simple model pays little attention to the electronic structure of atoms. In addition, the two-electron effects in atoms are weak and can essentially be described by the single active electron (SAE) approximation [3] together with the effect of the outer electron on the inner [4, 5].

  

Dynamics of molecules in strong laser fields are more complex and distinct since molecular ionization is generally accompanied by dissociation. Moreover, a molecule with an even number of electrons (hereafter referred to as an even-charge molecule and likewise for an odd-charge molecule) can dissociate into a symmetric (e.g. $A_2^{4+} \rightarrow A^{2+} + A^{2+}$) or asymmetric (e.g. $A_2^{4+} \rightarrow A^{+} + A^{3+}$) electronic configuration. These dissociation configurations can be correlated to the initial state of the parent molecule, i.e. the symmetric to the covalent (ground) state and the asymmetric to the ionic (excited) state of the parent molecule. The dissociation is also accompanied by a characteristic kinetic energy release. Every dissociation channel is identified by the charge on the respective fragments, $n$ and $m$. The internuclear separation at ionization, $R_{n,m}$, can be calculated by projecting the measured kinetic energy onto the potential energy (PE) curve of the particular molecular state. A study of the molecular ionization and dissociation, therefore, provides a wealth of information on the static and dynamic properties of the electronic structure of the molecule. Previous experimental and theoretical works on molecules have found an enhancement in ionization at a critical internuclear separation, $R_c$ [6–14], although the original concept of $R_c$ only applies to the ionization of odd-charge molecules such as $H_2^+$. For even-charge molecules, the symmetric dissociation configuration was regarded as dominant and the assumption was that the asymmetric channel was formed via a charge transfer transition from the symmetric channel [8]. Here, charge transfer refers to the process $A^{+q}A^{+q} \rightarrow A^{+q-1}A^{+q+1}$ as defined in [21].

There were several atypical observations, however, that motivated us to re-examine the existing view of molecular ionization. Although the enhancement of the ionization at $R_c$ was understood, how the molecule reaches $R_c$ from its initial equilibrium separation remains unexplained. In addition, many experiments have provided evidence of asymmetric dissociation channels [6, 15–19] and these channels appear to be formed at smaller internuclear separations than the symmetric channel [15, 20]. This suggests that the asymmetric channel is not necessarily formed from the symmetric channel. Further, the ionic (excited) states of the molecule (which dissociate via the asymmetric channel) couple strongly with the laser field. Kawata *et al* [21] were the first to show that these ionic states form the doorway to higher charge states of the molecule. In view of these anomalous findings, it becomes necessary to retrace the fundamental analytic methods. The basic questions that still remain are what strong field molecular dynamics information can be obtained from the characteristic $R_{n,m}$? And, if excited states of the molecule are indeed important, what is the mechanism for their population?

Recent work by Nibarger *et al* [22] involving a novel analysis of nitrogen molecules has shed some light on these basic questions. This analysis has revealed that the ionization process does, in fact, start at the equilibrium separation, $R_e$, and that ionization with ultrashort pulses is dominated by the asymmetric channels. In this paper, we present new data on the strong field ionization of iodine molecules and again find that the absence of a critical step in the simplest symmetric ionization pathway forces us to consider multi-electron effects in the ionization process. By extending the analysis to much higher charge states than in [22], we identify many distinct interactions leading to ionization and determine the dependence of each on the internuclear separation. Some of these interactions involve multiple electrons leading to two-electron ionization. Overall, we find that the ionization is dominated by pairs of states with gerade and ungerade ($g \leftrightarrow u$) symmetry and whose transition frequency is near resonant with the strong laser field. For a one-electron molecule, this pair contains the ground and first excited states of the molecule and can be represented as

$$\Psi_{g,u}^{1e} = \frac{(|a\rangle \pm |b\rangle)}{\sqrt{2}}. \tag{1}$$

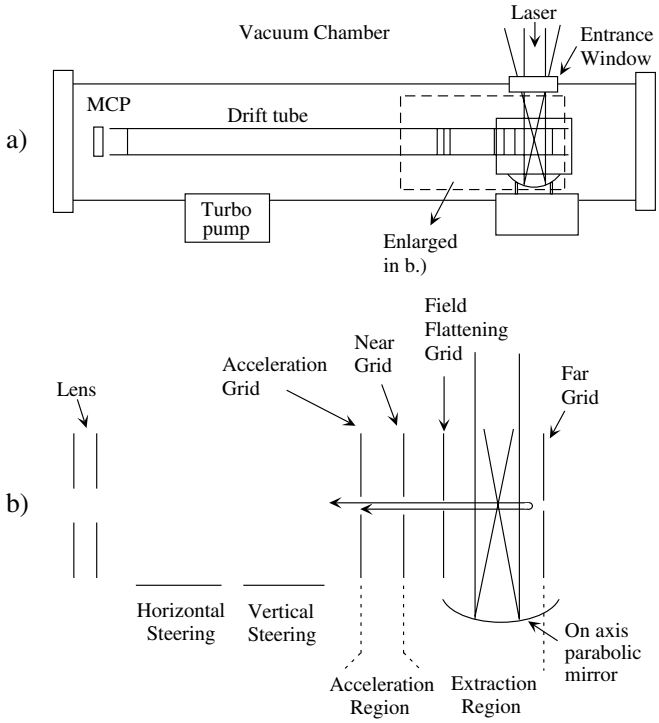


**Figure 1.** (a) Time of flight chamber. (b) Detail of electrostatic grids.

Here, $|a\rangle$ and $|b\rangle$ represent the electronic wavefunction centred on one well or the other. The dipole moment in this case is $\langle \Psi_g^{1e}|z|\Psi_u^{1e}\rangle \sim R/2$, where $R$ is the internuclear distance. In the case of a two-electron molecule, the lowest lying pair of ionic states dominates the ionization process and is represented as

$$\Psi_{g,u}^{2e,ionic} = \frac{(|a\rangle|a\rangle \pm |b\rangle|b\rangle)}{\sqrt{2}}, \tag{2}$$

with a dipole moment $\langle \Psi_g^{2e,ionic}|z|\Psi_u^{2e,ionic}\rangle \sim R$. In contrast, the covalent ground state is denoted by

$$\Psi_g^{2e,covalent} = \frac{(|a\rangle|b\rangle + |b\rangle|a\rangle)}{\sqrt{2}} \tag{3}$$

and is only weakly coupled to the ionic states at large $R$. Similar expressions are given in [21]. However, at large $R$ and for high charge states the molecular orbitals do not provide a good description of the two-electron wavefunction.

## 2. Experimental set-up

The laser system used for the experiment consists of a Kerr lens mode-locked Ti:sapphire oscillator and a multipass amplifier [23]. The output is 400 $\mu$J pulses at a 1 kHz repetition rate. The typical pulse duration is 33 fs with the centre wavelength at 800 nm.

The vacuum chamber (base pressure $<5 \times 10^{-10}$ Torr) used in the experiment has been described in detail previously [22]. It consists of a standard TOF geometry involving three regions (figure 1):

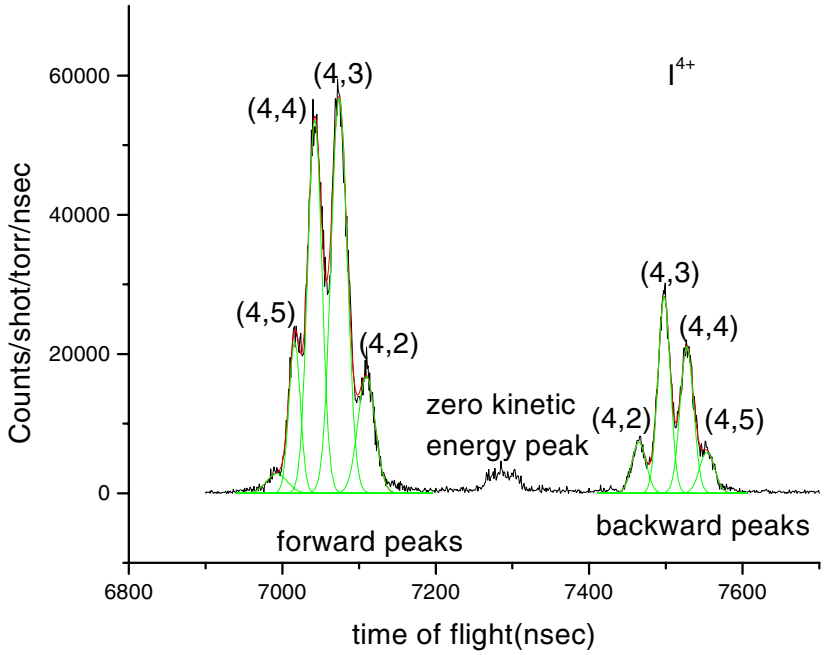


**Figure 2.** Typical TOF spectrum.
(This figure is in colour only in the electronic version)

(1) Extraction region: the laser pulses are focused here to $\sim$16 $\mu$m radius by an on-axis parabolic mirror to an intensity of up to $1.1 \times 10^{15}$ W cm$^{-2}$. Iodine gas is introduced effusively at a typical pressure of $10^{-6}$–$10^{-9}$ Torr and the ions are extracted by a dc field through a 1 mm aperture. An additional field-flattening grid is also used to minimize electrostatic lensing at the aperture.
(2) Acceleration region: here the extracted ions are given an additional acceleration. Symmetric TOF dispersion is achieved by adjusting the ratio of extraction to acceleration voltage.
(3) Drift tube: this is a 45 cm field-free region with a microchannel plate (MCP) at one end to detect the ions.

The signal from the MCP is amplified, discriminated and sent to a time-to-digital converter (TDC) which has a maximum time resolution of 0.5 ns.

A typical TOF spectrum is symmetric about the zero kinetic energy ion arrival time, as seen in figure 2, although the collection efficiency for the backward peak is smaller than that for the forward peak. Each peak corresponds to a specific dissociation channel: $(n, m)$ refers to the dissociation $I_2^{n+m} \rightarrow I^{n+} + I^{m+}$, with the first number, $n$, being the charge of the detected ion. The zero kinetic energy peak is due to the low field photodissociation of iodine molecules in the presence of an amplified spontaneous emission (ASE) pre-pulse [24]. These peaks can be greatly reduced by minimizing the ASE without affecting the molecular dissociation peaks, which are due to strong field ionization [15]. In order to obtain accurate kinetic energy measurements, detector saturation and space charge effects have to be minimized. For high pressures ($\sim 10^{-6}$ Torr), the number of ions in the focal region of the laser pulse is large, which creates space charge. In order to eliminate this effect, the TOF spectrum is taken at various pressures ($10^{-6}$–$10^{-9}$ Torr) and the measured kinetic energy is extrapolated to the limit of zero pressure.

## 3. Data analysis

The difference in arrival time ($\Delta t$) between the forward and backward peaks for a particular dissociation channel $(n, m)$ in the TOF spectrum is used to determine the total dissociation energy of that channel:

$$E_{n,m} = 2A(\Delta t)^2, \tag{4}$$

where $A = q^2F^2/8m$, $F$ is the dc electric field strength in the extraction region of the vacuum chamber (typical value $\sim 10^4$ V m$^{-1}$), $m$ is the mass of the fragment and $q$ is the charge of the fragment. In order to obtain the internuclear separation at ionization, $R_{n,m}$, the measured kinetic energy $E^{meas}_{n,m}$ is equated with the PE curve for the $(n, m)$ state:

$$E^{meas}_{n,m} = V_{n,m}(R_{n,m}) - V(\infty). \tag{5}$$

Here, $V$ can be adjusted such that $V(\infty) = 0$. Equation (5), however, does not take into account the kinetic energy accumulated from previous dissociation steps. Therefore, we modified equation (5) to include all such information, the details of which can be found in [22]. For any sequential or non-sequential ionization from $(i, j)$ to $(n, m)$, the equation can be generalized as

$$E^{meas}_{n,m} - E^{meas}_{i,j} = V_{n,m}(R_{n,m}) - V_{i,j}(R_{n,m}). \tag{6}$$

Coulomb PE curves do not account for the complex binding nature of molecules at small (1–3 Å) internuclear separations. Therefore, we use an approximate binding contribution, $V'_{n,m}(r)$, to the Coulomb curves:

$$V_{n,m}(r) = k\frac{nm}{r} - V'_{n,m}(r), \tag{7}$$

where $k$ is 14.4 eV Å, $r$ is in ångstroms and PE is in eV. Hence, equation (6) can be re-written as

$$\begin{aligned} E^{meas}_{n,m} - E^{meas}_{i,j} &= k\frac{nm}{R_{n,m}} - V'_{n,m}(R_{n,m}) - \left(k\frac{ij}{R_{n,m}} - V'_{i,j}(R_{n,m})\right) \\ &= k\frac{(nm - ij)}{R_{n,m}} - \Delta V'(R_{n,m}), \end{aligned} \tag{8}$$

where

$$\Delta V'(R_{n,m}) = V'_{n,m}(R_{n,m}) - V'_{i,j}(R_{n,m}). \tag{9}$$

The difference in binding energy between the various charge states is considerably smaller than the binding energy of the charge states themselves, i.e. $\Delta V'(R) \ll V'(R)$ [25,26]. Assuming $\Delta V' = 0$, equation (8) becomes

$$R_{n,m} = k\frac{(nm - ij)}{E^{meas}_{n,m} - E^{meas}_{i,j}}. \tag{10}$$

It is interesting to note that the internuclear separation at ionization for a particular channel is not dependent on that of the previous channel, only on its kinetic energy release. In this analysis, the effect of the Stark shift on the PE curves has been neglected. In order to test the accuracy of our analysis, we compared the experimentally obtained dissociation energy values of the (1, 1) channel of $N_2^{2+}$ to the field-free PE curves of $N_2^{2+}$ [22]. We found that, with the exception of the B $^3\Sigma_u^-$ state, every state is either bound at $R_e$ or dissociates with a kinetic energy value that is within our experimentally obtained range. Furthermore, a comparison of the time between ionization steps in $N_2$ with a 33 fs laser pulse showed that the ionization process closely follows the pulse, which is another indication that the analysis can reproduce

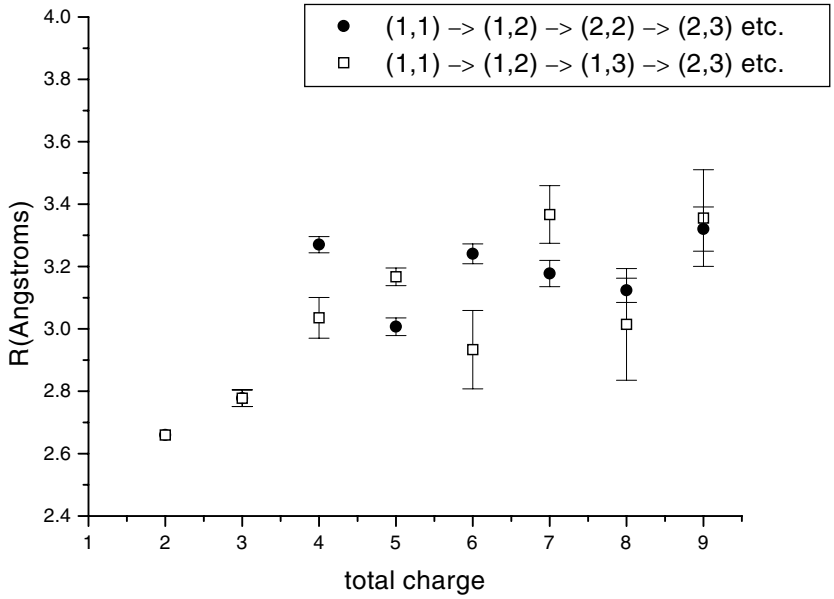


**Figure 3.** Internuclear separation at ionization (one-electron) for the symmetric and asymmetric pathways as a function of the total charge on the molecule. Error bars in our data reflect the uncertainty in $\Delta t$ (see equation (4)) determined by fitting the various peaks in the TOF spectrum (see figure 2, for example).

the molecular dynamics quite accurately. In the case of a heavy molecule like $I_2$, most of the kinetic energy gain occurs after the pulse when the effect of the Stark shift is negligible.

We applied equation (10) to our measured dissociation energies. In [22] it was reported that dissociation energy is a function of laser intensity and hence the data were analysed using two different methods: constant peak laser intensity and constant ion yield. Since the ionization has an onion shell-like transverse spatial structure [27], each ionization step occurs closer to the focus of the shell than the previous one. Each shell saturates a particular charge state. Because a high ion yield cut also corresponds to a point where a particular ionization has saturated, the two methods are nearly equivalent. In this paper, we have simply analysed the data using constant peak laser intensity.

One important consideration in our analysis is the expansion of the molecule as it interacts with the laser field: each step in the ionization process must occur at a larger $R$ as compared to the previous, i.e. $R_{n,m+1} > R_{n,m}$. Figure 3 shows $R_{n,m}$ as a function of the total charge on the molecule for both symmetric and asymmetric pathways up to $I_2^{9+}$. For each charge state, there are two values of $R_{n,m}$ shown; one corresponds to the ionization step involving an asymmetric channel and the other to the case where both channels are symmetric. For example, for a total charge of five, the symmetric value of $R_{n,m}$ corresponds to the $(2, 2) \rightarrow (2, 3)$ while the asymmetric value corresponds to the $(1, 3) \rightarrow (2, 3)$ ionization. From this figure, we have been able to map out the different one-electron ionization pathways. Figure 4 gives a complete picture of all such configurations. In addition, it also indicates the allowed (full arrow) and the unphysical (broken arrow) processes based on the requirement that $R_{n,m+1} > R_{n,m}$. Note that equation (10) always yields a value for $R_{n,m}$. Whether or not the value is physical depends on the internuclear separation of the preceding step. The implications of our observations are discussed in the next section.

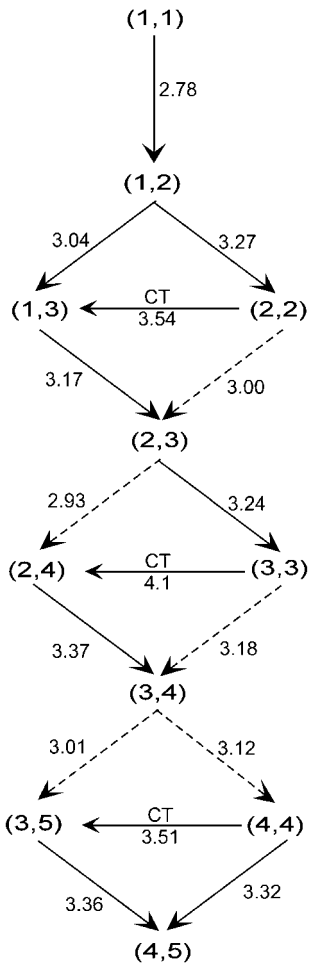


**Figure 4.** One-electron ionization pathways in molecular iodine. Numbers above arrows indicate $R$ (ångstroms) at ionization. CT = charge transfer. Full arrows are allowed configurations whereas the broken arrows are unphysical (see figure 3 for error bars).

## 4. Discussion

As the iodine molecule interacts with the laser field, it initially ionizes in an atom-like manner near the equilibrium internuclear separation ($R_e$) before reaching the repulsive curves of the higher charge states, which leads to dissociation of the molecule. This is a reasonable assumption to make since there is a good overlap between the ground state ($I_2$) and the lowest state of the singly ionized ($I_2^+$) iodine molecule [28]. The ionization therefore proceeds along vertical transitions with no change in the internuclear separation. Even though the (1, 0) dissociating channel is observed, it is small and can be attributed to bond softening [13,31,32]. Hence, (1, 1) is the first significant dissociation channel. Since the previous steps are non-dissociating, internuclear separation at ionization for (1, 1) cannot be calculated using equation (10). A calculation using the Coulomb approximation yields a value that is larger than the equilibrium internuclear separation ($R_e = 2.66$ Å). The same anomaly was noticed in the case of $N_2^{2+}$ by Nibarger *et al* [22] and it was resolved using known curves of $N_2^{2+}$.

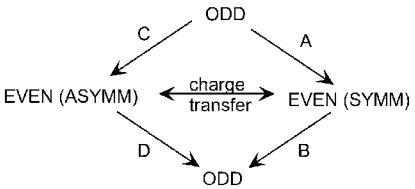


**Figure 5.** An ionization block showing the four different one-electron ionization pathways. Also included is the charge transfer process, which can change the values of $n$ and $m$ without ionization, i.e. $n, m \rightarrow n \pm 1, m \mp 1$.

**Table 1.** Types of one-electron ionization processes.

| Process | Initial charge state | Final charge state | Electrons ionized | No of active electrons | Example |
|---|---|---|---|---|---|
| A | Odd[a] | Even (symm.) | 1 | 1 | $(1, 2) \rightarrow (2, 2)$ |
| B | Even (symm.) | Odd | 1 | 2 | $(2, 2) \rightarrow (2, 3)$ |
| C | Odd | Even (asymm.) | 1 | 3[b] | $(1, 2) \rightarrow (1, 3)$ |
| D | Even (asymm.) | Odd | 1 | 2 | $(1, 3) \rightarrow (2, 3)$ |

[a] Here odd and even refer to the total charge on the molecule. Even (symm.) denotes the case where the charge is distributed equally between the two atoms while even (asymm.) denotes the case when there is a charge excess in one of the atoms as compared to the other.
[b] See discussion in text for explanation.

It turns out that ionization from $N_2^+$ to $N_2^{2+}$ is indeed a vertical transition at $R_e$. However, in the case of iodine, little is known about the PE curves of $I_2^{2+}$. We therefore have assumed that the same conclusion holds true for iodine as it does for nitrogen, i.e. (1, 1) is formed at $R_e$.

Once dissociation sets in, there are many different single-electron ionization processes accessible to the molecule (figure 4) and all such processes must be considered to form a complete picture of molecular ionization and dissociation. The electronic configuration of the initial and final charge states, the number of electrons involved in the interaction and the number of electrons ionized characterize the individual processes. As can be seen in figure 4, the diagram consists of smaller blocks that repeat up to higher and higher charge states and one such block is shown in figure 5. The processes within each block are summarized in table 1. Further, there is also the possibility of charge transfer between the symmetric and asymmetric states of an even-charged molecule.

Processes A and B were generally considered to be the dominant pathway in ionization and dissociation of molecules, i.e. all ionization proceeds via the symmetric channels [29, 30]. Process A was first studied in detail in the $H_2^+$ molecule and it led to the concept of enhanced ionization at $R_c$ [12]. In the presence of the laser field, an electron in the upper well of the molecular potential can easily tunnel through the small internal barrier, thereby leading to high ionization rates (figure 6). An electron localized in the upper well represents an excited state of the molecule and can be populated through resonant excitation or electron trapping and localization. In both cases, the strong gerade–ungerade (g $\leftrightarrow$ u) coupling in the potential plays an important role [12]. This coupling also gives rise to the phenomena of bond softening and hardening [13, 31–34]. In our data, ionization from $(1, 2) \rightarrow (2, 2)$ and $(2, 3) \rightarrow (3, 3)$ falls under this category. Hence, we would expect (2, 2) and (3, 3) to be formed at $R_c$ for iodine and, as seen from figure 3, it is indeed so. The value of $R_c$ obtained from our experiment ($\sim$3.3 Å) is in good agreement with those obtained by Posthumus *et al* [35] using a 55 fs pulse. In addition, $(1, 0) \rightarrow (1, 1)$ ionization will not show such an enhancement due to strong binding at small $R$.

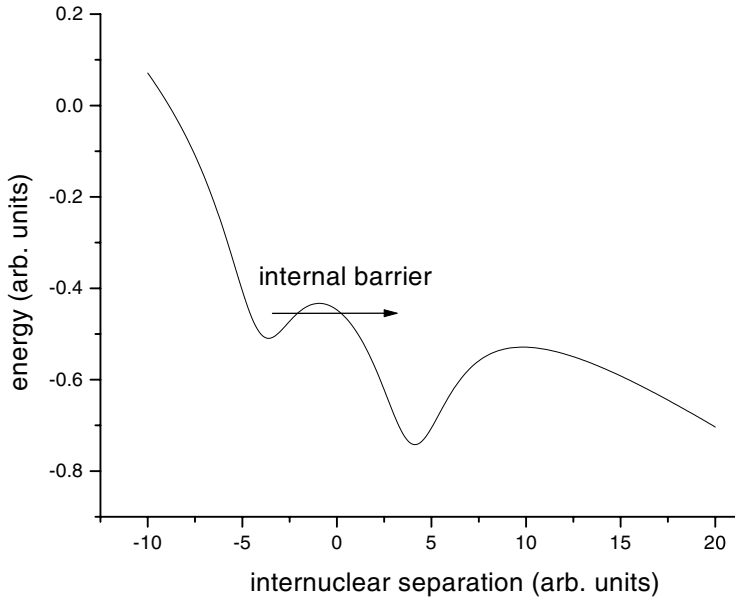


**Figure 6.** Schematic of process A where the electrons in the upper well tunnel through the small internal barrier at $R_c$.

Process B is more complicated since it involves ionization of an even-charge molecule with two active electrons. In our data, ionization from $(2, 2) \rightarrow (2, 3)$ would be representative of this process. The most surprising result from our iodine data and previous work on nitrogen [22] is that this process is unphysical, based on the requirement that $R_{n,m+1} > R_{n,m}$. In fact, this anomaly was first recognized by Cornaggia *et al* [6] a decade ago using a simple Coulomb model. Kawata *et al* [21] were the first to address this process in the $H_2$ molecule and they found that enhanced ionization does exist for this configuration primarily due to the field-induced avoided crossings between the covalent and ionic molecular states. While the analysis may be true for lower charge states ($Z = 1$), their results need not scale to higher ones, where we find that ionization from the ground covalent state does not occur. This may be because the electronic structure of an even-electron system changes significantly with $Z$. For example, in figure 7, for a 1D model molecule, $A_2^{4+}$ ($Z = 3$), the excited ionic states lie well below the excited covalent states[3] while for $H_2$ ($Z = 1$), these states are strongly mixed [21]. We therefore believe that the model developed by Kawata *et al* may not apply to the charge states

[3] The PE curves shown in figure 7 were obtained from the following Hamiltonian:

$$H(x_1, x_2) = \frac{-Z}{\sqrt{(x_1 - R/2)^2 + a^2}} + \frac{-Z}{\sqrt{(x_1 + R/2)^2 + a^2}} + \frac{-Z}{\sqrt{(x_2 - R/2)^2 + a^2}} + \frac{-Z}{\sqrt{(x_2 + R/2)^2 + a^2}} + \frac{1}{\sqrt{(x_1 - x_2)^2 + a^2}} - \frac{1}{2}\frac{\partial^2}{\partial x_1^2} - \frac{1}{2}\frac{\partial^2}{\partial x_2^2}$$

where $a = 0.742$. All quantities are in atomic units. Schrödinger's equation:

$$\mathrm{i}\frac{\partial}{\partial t}\Psi(x_1, x_2) = H\Psi(x_1, x_2),$$

was integrated in imaginary time on a spatial grid to find the ground state. Excited states were obtained in the same way, except that lower lying states were projected out at each step of the integration. The correct spatial symmetry (symmetric for the singlet states) was imposed at every time step.

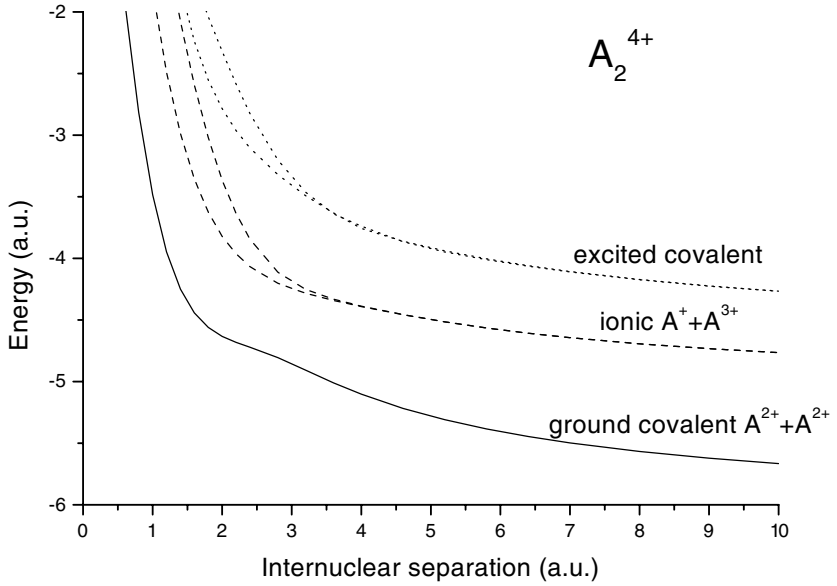


**Figure 7.** Covalent and ionic PE curves of a 1D molecule calculated using the procedure (see footnote 3). The ground covalent state of the molecule is represented by the full curve, the lowest lying ionic states by the broken curves and the excited covalent states by the dotted curves.

that we measure. In any case, we find that process B is not detected and does not lead to higher charge states of the molecule as expected from [21]. This is an important observation since it implies the breakdown of the well accepted model for molecular ionization [29, 30].

The above observation raises the important question: if process B is not dominant, how then does the ionization proceed? This question is especially important, as any other ionization configuration leading to higher charge states would involve multi-electron interactions and this has never been considered before. Since process B is absent, we consider ionization via $(1, 2) \rightarrow (1, 3)$ (process C). It turns out that process C is indeed allowed by our criterion and, further, it gives an internuclear separation that is smaller than that of the $(1, 2) \rightarrow (2, 2)$ ionization. This is significant for three reasons:

(a) it implies (1, 3) is not formed via a charge transfer from (2, 2) as was previously assumed [8];
(b) (1, 3) is formed as a result of direct ionization from (1, 2); and
(c) it proves the asymmetric channel dominates the ionization process in the ultrashort pulse regime.

In fact, Nibarger *et al* [22] were the first to show the importance of process C and our data on $I_2$ are consistent with these results. Since process C is crucial to reaching higher charge states of the molecule, it is important to study the dynamics of the $(1, 2) \rightarrow (1, 3)$ ionization. The final charge state (1, 3) of this process is a configuration consisting of two active electrons in the outermost orbitals of the $I^{1+}$ atom plus the electron that has been ionized from the $I^{2+}$ atom. This necessarily implies that the $(1, 2) \rightarrow (1, 3)$ ionization involves three active electrons, making it hard to model. Moreover, the exact mechanism of populating the excited ionic state correlating to the (1, 3) dissociation channel is not known. We believe that the (1, 2) state ionizes in a manner similar to rescattering in atoms. The (1, 2) molecular configuration consists of a pair of states with $g \leftrightarrow u$ symmetry that couple strongly to the laser field. This leads to

**Table 2.** Two-electron ionization processes.

| Process | Initial charge state | Final charge state | Electrons ionized | No of active electrons | Example |
|---|---|---|---|---|---|
| E | Even (asymm.) | Even (symm./asymm.) | 2 | 4 | $(1, 3) \rightarrow (2, 4)/(3,3)$ |
| F | Even (symm.) | Even (symm./asymm.) | 2 | 4 | $(2, 2) \rightarrow (2, 4)/(3,3)$ |
| G | Odd | Odd | 2 | 3 | $(1, 2) \rightarrow (2, 3)$ |

electron localization that alternates between the two wells as a function of the laser field. The inner electron experiences an altered potential due to the motion of the strongly driven outer electron, thereby leading to its ionization ('internal rescattering') [21]. The ionization of an inner electron can then leave the molecule in an excited state, in this case the ionic state (1, 3). This is in contrast to the case of atoms where the outer electron is ionized and then returns to the core due to the laser field leading to the ionization of the inner electron [5].

Regardless of the mechanism of population, process C leads to the formation of the ionic excited state of the even-charged molecule. This state is, in fact, a pair of strongly coupled g $\leftrightarrow$ u states similar to those of $H_2^+$ but with twice the dipole moment (see equations (1) and (2)). Hence, there is a strong interaction with the laser field, which appears to cause further ionization to higher charge states (process D). Ionization from $(1, 3) \rightarrow (2, 3)$ falls under this class and is consistent with our data. In addition, the (1, 3) could also convert to the (2, 2) through a charge transfer process.

The processes described so far involve one-electron ionization and it is generally considered to be the dominant ionization process in both atoms and molecules. Unlike previous data on $N_2$, we have been able to extend our analysis to higher charge states of $I_2$. From this, we can infer the dependence of the ionization pathways on the internuclear separation. Consider the second ionization block in figure 4: on the symmetric side, the results remain the same, i.e. the (2, 3) state can ionize to (3, 3) but further ionization from (3, 3) is unphysical (process B). This further supports our argument that ionization from the ground covalent state is not a dominant process. Another important aspect of this block is that neither is the ionization from (2, 3) to (2, 4) the principal pathway to higher charge states as expected from the discussion above. This process may only be dominant at small $R$. Nevertheless, this now leaves a complete gap in the pathway and there appears to be no way to connect the (2, 4) and higher charge states to the lower ones. The (2, 4) state can, in principle, be formed from the (3, 3) via a charge transfer. From our data, we find that this occurs at a internuclear separation of $\sim$4 Å, which implies that the single-electron ionization pathway from $(2, 4) \rightarrow (3, 4)$ is now not viable based on $R_{n,m+1} > R_{n,m}$. In general, we find that charge transfer processes could only occur at large internuclear separations and therefore rule out all symmetric $\rightarrow$ asymmetric charge transfer processes in our data. Given this, we find it necessary to consider the next higher-order process, i.e. two-electron ionization (figure 8). This is significant since the two-electron ionization rate is typically small in atoms while in molecules it would appear, under certain conditions, that the two-electron ionization rate can exceed the one-electron rate. The higher charge states can be accessed via a double ionization in three ways: processes E, F and G and are enumerated in table 2.

Process G would lead to the higher charge state (3, 4) but is not sufficient to form a complete picture since it cannot access states (2, 4), (3, 5) or (4, 4). In addition, double ionization from (3, 3) to (4, 4) or to (3, 5) is unphysical based on $R_{n,m+1} > R_{n,m}$ (process F). Therefore, process E, $(1, 3) \rightarrow (2, 4)$, is the only pathway that is consistent with our data

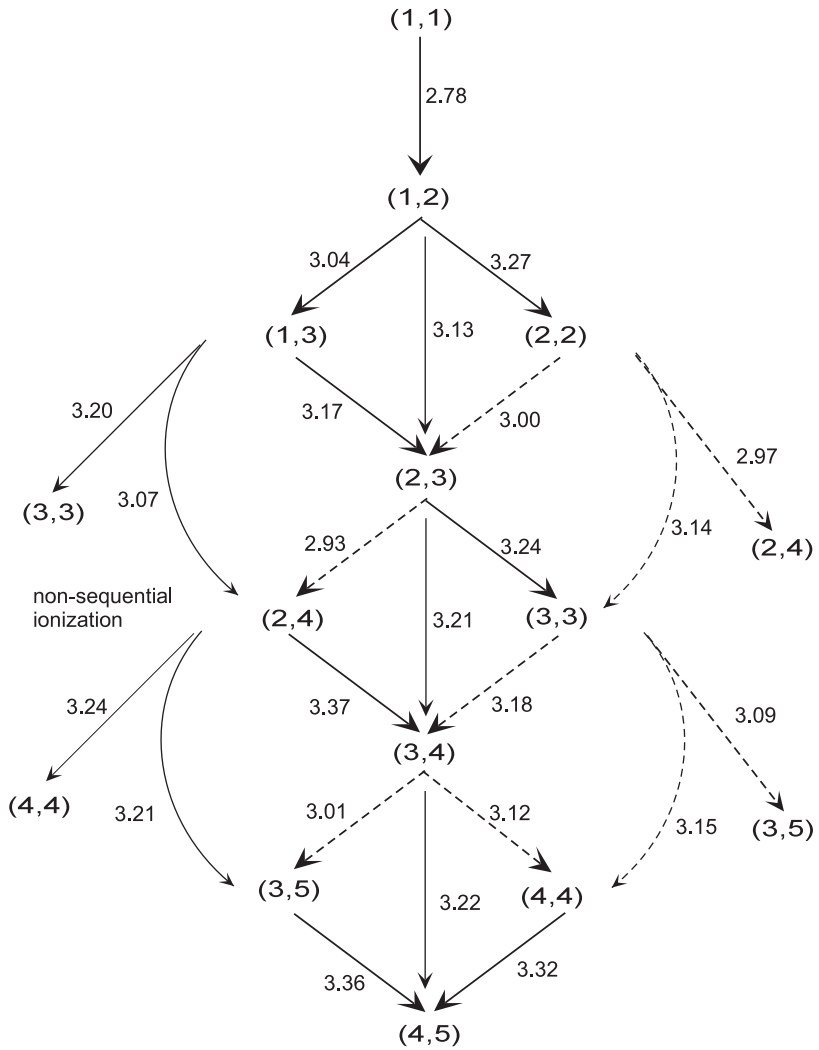


**Figure 8.** One- and two-electron ionization pathways in molecular iodine.

and provides a link to higher ionization blocks via process D. Thus we see that, in order to access any of the higher charge states, it not only becomes necessary to consider higher-order processes (two-electron ionization), but, in particular, two-electron ionization from the ionic state of the molecule (process E). This observation provides further evidence that ionization is dominated by states that have strong coupling to the laser field. The gap between these levels is on the order of the laser frequency and much smaller than their detuning from the ground covalent state. The laser field strongly drives such states and can evidently give rise to double ionization.

An analysis of the last block in figure 4 indicates that, as the internuclear separation increases, the number of allowed one-electron ionization configurations becomes fewer. The important change in this block is that process A is no longer viable as the molecule may have expanded beyond $R_c$. Process B, $(4, 4) \rightarrow (4, 5)$, is hard to interpret as it is not clear where the (4, 4) comes from and process C is also not seen, perhaps due to the same reasons as

stated previously. This implies that double ionization has to be evoked, yet again, in order to explain the observation of the higher charge states. We find that process E can connect this block to the preceding one, while process F turns out to be unphysical once more.

From the above discussion, we observe that the ionic states of the molecule dominate the ionization process even up to higher charge states and large $R$. The gerade and ungerade components of the ionic states are near resonant with the laser field, which leads to a strong coupling with the field whereas the covalent ground state exhibits weak coupling. This strong coupling can sustain both single- and multi-electron processes and it proves to be a very efficient way to ionize to higher charge states. The ionic state can be correlated to the asymmetric dissociation channel of the parent molecule and the covalent ground state to the symmetric dissociation channel. In other words, any state that couples strongly to the laser field dissociates via the asymmetric channel.

## 5. Conclusions

Ionization pathways in iodine molecules were studied with a view to obtaining more insight into molecular dynamics. A study of the characteristic internuclear separation at ionization, $R_{n,m}$, has revealed many distinct configurations into which a molecule can ionize. These configurations can be classified into two types, depending on the nature of the interaction with the laser field: strong-coupled and weak-coupled. The strong-coupled configurations dominate the ionization process and lead to higher charge states while the weak-coupled configurations play a much smaller role. We have also found that the relative importance of these configurations depends on the internuclear separation, and eventually only those that couple strongly to the laser field survive. Finally, a complete picture of molecular ionization and dissociation in strong laser fields is obtained only when two-electron ionization is considered. In this paper, we have developed a framework for molecular dynamics that has, for the first time, detailed all the possible ionization configurations and provided a viable and consistent pathway for the ionization process.

## Acknowledgments

We would like to acknowledge support from the NSF under grant no PHY-9987804. GNG was also supported through funding as a Cottrell Scholar of the Research Corporation.

## References

[1] Gavrila M 1992 *Atoms in Intense Laser Fields* (New York: Academic)
[2] Ammosov M V, Delone N B and Krainov V P 1986 *Sov. Phys.–JETP* **64** 1191
[3] Kulander K, Shafer K and Krause J 1992 *Atoms in Intense Laser Fields* (New York: Academic)
[4] Watson J B, Sanpera A, Lappas D G, Knight P L and Burnett K 1997 *Phys. Rev. Lett.* **78** 1884
[5] Corkum P 1993 *Phys. Rev. Lett.* **71** 1994
[6] Cornaggia C, Lavancier J, Normand D, Morellec J, Agostini P, Chambaret J and Antonetti A 1991 *Phys. Rev.* A **44** 4499
[7] Seideman T, Ivanov M Yu and Corkum P B 1995 *Phys. Rev. Lett.* **75** 2819
[8] Posthumus J, Codling K, Frasinski L and Thompson M 1997 *Laser Phys.* **7** 813
[9] Barnett R and Gibson G N 1993 *Phys. Rev.* A **59** 4843
[10] Bandrauk A D and Hengtai Y 1999 *Int. J. Mass Spectrosc.* **192** 379
[11] Chelkowski S and Bandrauk A D 1995 *J. Phys. B: At. Mol. Opt. Phys.* **28** L723
[12] Zuo T and Bandrauk A D 1995 *Phys. Rev.* A **52** R2511
[13] Gibson G, Li M, Guo C and Neira J 1997 *Phys. Rev. Lett.* **79** 2022
[14] Constant E, Stapelfeldt H and Corkum P B 1996 *Phys. Rev. Lett.* **76** 4140

[15] Gibson G N, Li M, Guo C and Nibarger J P 1998 *Phys. Rev.* A **58** 4723
[16] Guo C, Li M and Gibson G N 1999 *Phys. Rev. Lett.* **82** 2492
[17] Boyer K, Luk T S, Solem J C and Rhodes C K 1989 *Phys. Rev.* A **39** 1186
[18] Strickland D T, Beaudoin Y, Dietrich P and Corkum P B 1992 *Phys. Rev. Lett.* **68** 2755
[19] Posthumus J H, Giles A J, Thompson M R and Codling K 1996 *J. Phys. B: At. Mol. Opt. Phys.* **29** 5811
[20] Hishikawa A, Iwamae A, Hoshina K, Kono M and Yamanouchi K 1998 *Chem. Phys. Lett.* **282** 283
[21] Kawata I, Kono H, Fujimura Y and Bandrauk A D 2000 *Phys. Rev.* A **62** 031401-1
[22] Nibarger J P, Menon S V and Gibson G N 2001 *Phys. Rev.* A **63** 053406
[23] Li M and Gibson G N 1998 *J. Opt. Soc. Am.* B **15** 2404
[24] Normand D and Schmidt M 1996 *Phys. Rev.* A **53** R1958
[25] Corkum P B, Ivanov M Y and Wright J S 1997 *Ann. Rev. Phys. Chem.* **48** 387
[26] Wright J, DiLabio G, Matusek D, Corkum P, Ivanov M Y, Ellert C, Buenker R, Alekseyev A and Hirsch G 1999 *Phys. Rev.* A **59** 4512
[27] Schmidt M, Dobosz S, Meynadier P, D'Oliveira P, Normand D, Charron E and Suzor-Weiner A 1999 *Phys. Rev.* A **60** 4706
[28] Li J and Balasubramanian K 1989 *J. Mol. Spectrosc.* **138** 162
[29] Codling K, Frasinski L J and Hatherly P A 1989 *J. Phys. B: At. Mol. Opt. Phys.* **22** L321
[30] Hatherly P A, Stankiewicz M, Codling K, Frasinski L J and Cross G M 1994 *J. Phys. B: At. Mol. Opt. Phys.* **27** 2993
[31] Zavriyev A, Bucksbaum P, Muller H and Schumacher D 1990 *Phys. Rev.* A **42** 5500
[32] Zavriyev A, Bucksbaum P, Squier J and Saline F 1993 *Phys. Rev. Lett.* **70** 1077
[33] Yao G and Chu S 1993 *Phys. Rev.* A **48** 485
[34] Frasinski L J, Posthumus J H, Plumridge J, Codling K, Taday P F and Langley A J 1999 *Phys. Rev. Lett.* **83** 3625
[35] Posthumus J H, Giles A J, Thompson M R, Shaikh W, Langley A J, Frasinski L J and Codling K 1996 *J. Phys. B: At. Mol. Opt. Phys.* **29** L525